Synthesis of metal-bis-(β-diketones) complexes and anti-microbial evaluation study

Mohobe Pooja[1], Pandhurnekar Chandrashekhar[2]*, Pandhurnekar Himani[1] and Bhattacharya Doyel[1]
1. Department of Chemistry, Dada Ramchand Bakhru Sindhu Mahavidyalaya, Nagpur, Maharashtra, 440 017, INDIA
2. Department of Chemistry, School of Humanities and Basic Sciences, Shri Ramdeobaba College of Engineering and Management, Ramdeobaba University, Nagpur, Maharashtra, 440 013, INDIA
*pandhurnekarcp@rknec.edu

Abstract

In the present work, β-diketone ligands, namely, 1-(2,4-dihydroxy-5-nitrophenyl)-3-p-tolylpropane-1,3-dione, were synthesized. Different metal transition complexes for cobalt (II), nickel (II), manganese (II), copper (II) and zinc (II) have been successfully synthesized. The β-diketone ligand is afforded by the Baker–Venkataraman rearrangement of 4-hydroxy-5-nitro-2-p-tolyloxyacetophenone. The synthesized ligands were characterized by elemental analysis, Fourier transform infrared (FT-IR) spectroscopy, 1H-nuclear magnetic resonance (^{1}H-NMR) spectroscopy and mass spectrometry for structural confirmation. All the newly synthesized metal complexes were characterized by their physical properties, elemental analyses, FT-IR spectra, electronic and magnetic spectra and thermogravimetric analysis. The obtained results show that the newly synthesized materials are stable and have decomposition temperatures in the range of 420–570 ^{0}C.

Furthermore, to analyze their microbial potency, the antibacterial activity of the newly synthesized metal complexes was tested against Gram-positive (Bacillus subtilis and Staphylococcus aureus) and Gram-negative (Escherichia coli, Pseudomonas aeruginosa and Proteus vulgaris) bacterial strains. Some of the complexes have shown promising activities against specific bacterial strains; thus, it can be concluded that metal complexes with β-diketones can be used as antimicrobial agents in the future.

Keywords: β-diketone ligands, Metal Complex, Biological Activity, Gravimetry Analysis.

Introduction

β-diketones, also known as 1,3-diketones, play a crucial role in medicinal chemistry[4,12,14]. In recent decades, organic, inorganic, environmental and physical chemists have been strongly influenced by β-diketones, also known as β-dicarbonyl molecules. They serve as essential building blocks for synthesizing core heterocycles like pyrazole, isoxazole, triazole, chromene, coumarin, pyrimidine, pyridine, pyrazole, thiazole and thiophene. Additionally, these compounds act as valuable chelating ligands for various lanthanide and transition metals in material science[19]. Natural sources such as eucalyptus leaves, liquorice roots, vanilla beans and sunflower pollen contain β-diketones. Dibenzoylmethane (DBM) and n-tritriacontane-16, 18-dione (TTAD) are examples of naturally occurring β-diketones with potent antioxidant and anticancer properties[18].

β-Diketones are mainly classified on the basis of their structure as linear β-diketones, cyclic β-diketones or double-bonded β-diketones[10]. The presence of a β-carbonyl group with at least one proton on the second carbon atom allows tautomeric equilibrium of the keto and enol forms. A wide range of variables, including solvent, temperature and the presence of other species that can form hydrogen bonds, affect the keto-enol equilibrium[9]. The coordination behavior of β-diketones also significantly influences the relative stabilities of the β-diketone complexes as well as their use in biomedicine[20]. Additionally, owing to the presence of simple keto-enol tautomerism caused by a single-bond CH_2 group separating the diketo moiety, β-diketones are promising scaffolds for drug delivery and discovery.

Researchers have made significant advances in β-diketone synthesis over the last decade[2]. Various chemical methods (Claisen condensation, the hydration of alkynones and decarboxylative coupling) and catalytic approaches (bio-catalysis, organo-catalysis and metal-based catalysis) have been explored. β-Diketonate compounds are highly important in the field of medicinal chemistry since they exhibit various biological activities[11]. β-Diketone compounds also have hepatoprotective and nephroprotective activity and have hypoglycemic and antirheumatic properties[7].

Some β-diketone compounds are also beneficial for the prevention and treatment of several CNS diseases such as Alzheimer's disease, Parkinson's disease and tumors. Owing to the diverse properties of β-diketones, phenolic hydroxyl groups, nitro groups etc., the synthesis of new β-diketone compounds and their transition metal complexes is thought worthwhile. Earlier, we synthesized and studied the properties of 1-(2,4-dihydroxy-5-nitrophenyl)-3-(thiophen-2-yl)propane-1,3-dione and its metal complexes. These metals complexes were subjected to the anti-microbial study. It was observed that such complexes have moderate to good potency towards different microbes[17].

Considering these facts, we herein report the synthesis of β-diketone ligands. The ligand 1-(2,4-dihydroxy-5-nitrophenyl)-3-p-tolylpropane-1,3-dione was further used for the synthesis of different metal transition complexes for

https://doi.org/10.25303/301rjce020030

cobalt (II), nickel (II), manganese (II), copper (II) and zinc (II). Their biological activities have also been tested.

Material and Methods

Anhydrous acetates of copper (II), cobalt (II), manganese (II), nickel (II) and zinc (II) of analytical reagent grade were used for the complexation of ligand. All the chemicals used for the synthesis of ligand as well as metal complexes were of analytical reagent grade of Sigma-Aldrich or Merck, India. These were used without further purification. Solvents such as ethanol, dimethyl sulfoxide and dimethylformamide of Loba Chemicals, India (AR Grade) used were purified by fractional distillation method and only middle fractions were used for the present study.

The infra-red spectra of the ligand and complexes were recorded on Shimandzu spectrophotometer FTIR-8101A using KBr pellets. They have been examined in the region 400-4000 cm^{-1}. The NMR spectra of ligand and metal complexes were recorded on Brucker AC-300 F (300 MHz) NMR spectrometer by using DMSO-d^6, D_2O and $CDCl_3$ as solvents and tetramethylsilane as an internal standard. UV-Vis absorption spectra were recorded on UV-VIS-NIR Spectrophotometer Model Lambda 750 Perkin Elmer. The powdered samples of metal complexes were scanned in the region of 200-1000 nm. All the spectral assignments are based on the earlier calculations of Tanabe, Sugano and Orgel. Thermogravimetric studies were carried out on Perkin Elmer SII, Diamond TG/DTA Thermogravimetric analyzer on Diamond TG/DTA instrument. The samples were heated in air as medium. X-ray diffraction of complexes were recorded using Pan analytical X-ray diffractometer (Philips, Holland) using nickel filtered Cu-Kα radiation ($\lambda = 1.5418$ Å).

Synthesis of 2-acetyl-5-hydroxy-4-nitrophenyl acetate (HNTO) (Compound 3): The synthesis of 1-(2,4-dihydroxy-5-nitrophenyl)ethan-1-one (2) from 2′,4′-dihydroxyacetophenone (1) has been done as per literature method reported earlier[28]. 0.02 mol of 1-(2,4-dihydroxy-5-nitrophenyl)ethan-1-one (2) and 0.02 mol of p-toluic acid were dissolved in 10 ml of dimethylformamide and cooled in an ice bath. Then, 3 ml of $POCl_3$ was added dropwise with constant stirring and the temperature was maintained below 100 ^{0}C. After 2 h, the reaction mixture was poured on crushed ice with stirring. The white solid mixture was separated and then washed with cold water. The product was filtered and recrystallized from alcohol. Yield: 66%; m.p.: 65 ^{0}C

Synthesis of 1-(2,4-dihydroxy-5-nitrophenyl)-3-(p-tolyl)propane-1,3-dione (DNTD) (Compound 4): 0.02 mol of 2-acetyl-5-hydroxy-4-nitrophenyl acetate (3) was dissolved in approximately 18 ml of dry dimethyl sulfoxide in a 50 ml bolt-necked flask and heated to 50 ^{0}C. Potassium hydroxide (0.03 mol) was added with mechanical stirring and the mixture was powdered rapidly in a mortar preheated in an oven at 100 ^{0}C and stirred for 15 min. The reaction mixture was then cooled to room temperature and acidified by adding 25 ml of 10% aqueous acetic acid with stirring. The yellow-colored compound obtained was filtered and recrystallized from ethanol. Yield: 87%; m.p. 150 ^{0}C.

Synthesis of the bis[1-(2,4-dihydroxy-5-nitrophenyl)-3-(p-tolyl)propane-1,3-dione)] metal complex (Compound 5a-5e): Complexes of 1-(2,4-dihydroxy-5-nitrophenyl)-3-(p-tolyl)propane-1,3-dione (4) were synthesized by dissolving the ligand (0.04 mol) and acetate of metal (0.02 mol) in a 2:1 molar ratio in ethanol. The olive-colored solid 5a precipitate was filtered and washed with hot ethanol.

Antibacterial screening: The antimicrobial activities of all the compounds were determined via the filter paper disc diffusion method. The synthesized compounds were screened against pathogenic bacteria such as *S. aureus* ATCC (25925), *P. vulgaris* NCL (2388), *P. aeruginosa* NCL (2200), *E. coli* ATCC (25922) and *B. subtilis* NCL (2185) via the filter paper disc diffusion method. The antibiotic drugs ampicillin, gentamicin and erythromycin were used as reference drugs. 2 gm of compound was taken and mixed well with 5 ml of the solvent (Chloroform). The contents were filtered next day and thus, the filtrate coming out is the extract of the compound in the solvent. The selected pathogenic bacteria were maintained on nutrient agar media for 36 hrs.

For the preparation of nutrient agar media, 0.5 gm peptone, 0.3 gm beef extract, 1.5-2.0% agar at pH 7.0 were mixed well, agar and autoclave were dissolved and after it, the plates were poured accordingly. For the preparation of broth culture, 10 ml nutrient broths were taken in five tubes and sterilized by autoclaving. The tubes were cooled and the loops full of respective culture were inoculated in their tubes. The tubes were kept in an incubator for 24 hours at 37 ^{0}C. The bacterial cultures were inoculated into nutrient broth and incubated at 37 ^{0}C on a rotary shaker at 100 rpm. After 36 hrs of incubation, the bacterial suspensions were used for further tests. 25 clean dry and sterilized Petri plates were taken and labeled with the name of organism and also the extract used.

The nutrient agar was liquefied and poured in a water bath and cool to 50 ^{0}C. From the broth culture, 5 ml of the culture was taken and mixed well with the liquefied nutrient agar. The content was poured into the plate. After the media has solidified, the sterile disk was picked up with the lightly flamed forceps, the disk was dipped half way into a beaker of the extract and a disk in the center of the medium was placed. To secure the disk to the medium, press it slightly with the forceps. The plate at 37 ^{0}C was incubated for 36 hours. The zone of inhibition surrounding the disk was observed and recorded. Antibacterial activity was then carried out with 100 µg/mL synthesized compounds. Filter paper discs soaked in solvent (chloroform) were used as negative controls, while the discs soaked in standard broad-spectrum antibiotic solutions (ampicillin, gentamicin and erythromycin) were used as positive controls.

Results and Discussion

Chemistry: Metal-beta-diketone complexes of cobalt, nickel, manganese, copper and zinc were prepared using 1-(2,4-dihydroxy-5-nitrophenyl)-3-(p-tolyl)-propane-1,3-dione (4) by stoichiometrically reaction of metal:ligand ratio equal to 1:2 as depicted in fig. 1. The yield and color of the synthesized complexes are given in table 1. The %Yield of complexes varies in the range of 74% up to 90%. The experimental data of the elemental analysis was observed to be in good agreement to the calculated values of percentages of C,H,N and metal in the complexes as collected in table 1.

Table 1
Appearance, yield and elemental analyses of newly synthesized compounds.

Name of complexes	**Color**	**Yield (%)**	**Elemental Analyses**							
			Found (%)				**Calculated (%)**			
			C	H	N	M	C	H	N	M
HNTO	Yellow	66	47.64	4.72	4.60	--	48.25	4.31	4.44	--
DNTD	Lemon green	87	48.21	4.66	4.05	--	48.25	4.31	4.44	--
$Mn(DNTD)_2.2H_2O$	Orange red	81	54.00	4.24	3.54	6.99	53.26	4.16	3.88	7.62
$Co(DNTD)_2.2H_2O$	Rust	74	53.66	4.52	3.88	8.14	52.96	4.14	3.86	8.13
$Ni(DNTD)_2.2H_2O$	Gambage orange	83	52.48	4.55	3.84	8.31	52.96	4.14	3.86	8.09
$Cu(DNTD)_2$	Olive	90	55.83	3.54	4.21	9.02	55.33	3.75	4.03	9.15
$Zn(DNTD)_2$	Golden white	81	55.64	3.46	3.69	8.87	55.25	3.74	4.03	9.40

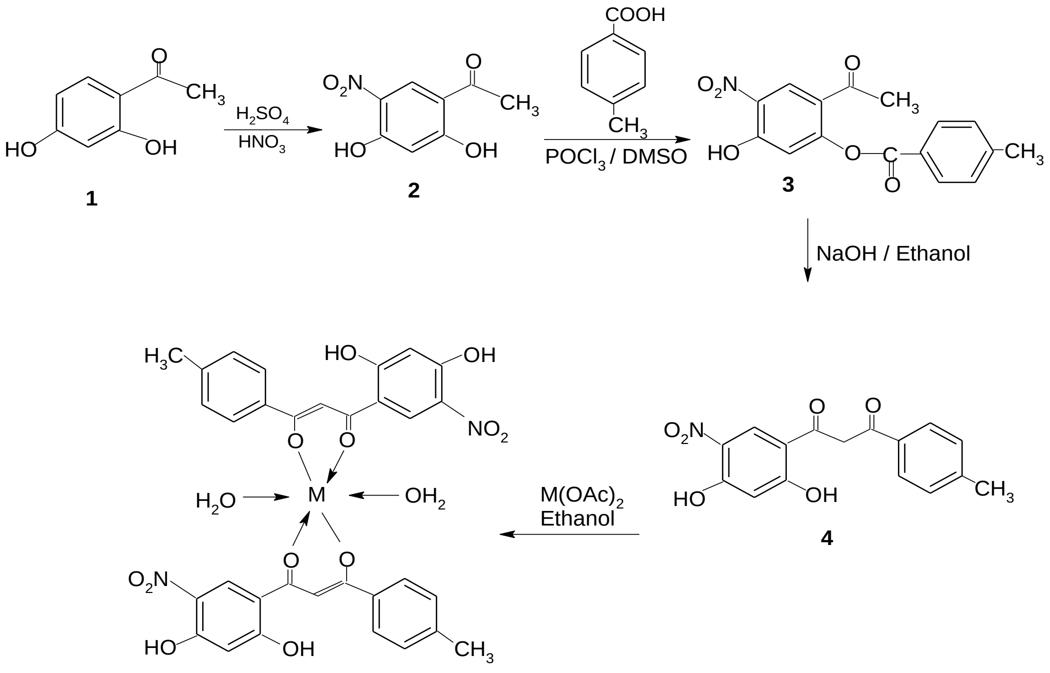

Figure 1: Synthesis of the ligand and its metal complexes.

Table 2
Infrared data of ligand and its metal complexes (in cm^{-1})

Compound	**C=O**	**C=C**	**-C-O Phenolic**	**-C-H Aromatic**	**>CH Alip**	**-OH Phenolic**	**-C-O Enolic**	**-C-CH_3**	**M-O**	**M-H_2O Coordinated water**	**C-NO_2**	**-CH_3**
HNTO	1691	1610	1184	3054	2918	3462	1196	2876	--	--	1545	2970
DNTD	1682	1606	1202	3056	2918	3459	1202	2878	--	--	1528	--
$Mn(DNTD)_2.2H_2O$	1608	1577	1200	3056	2932	3430	--	2863	439	762	1488	--
$Co(DNTD)_2.2H_2O$	1616	1591	1221	3032	2922	3430	--	2879	411	765	1488	--
$Ni(DNTD)_2.2H_2O$	1621	1569	1189	3053	2923	3430	--	2866	462	768	1492	--
$Cu(DNTD)_2$	1618	1586	1208	3072	2922	3430	--	2871	426	--	1492	--
$Zn(DNTD)_2$	1617	1582	1198	3008	2916	3430	--	2868	470	--	1488	--

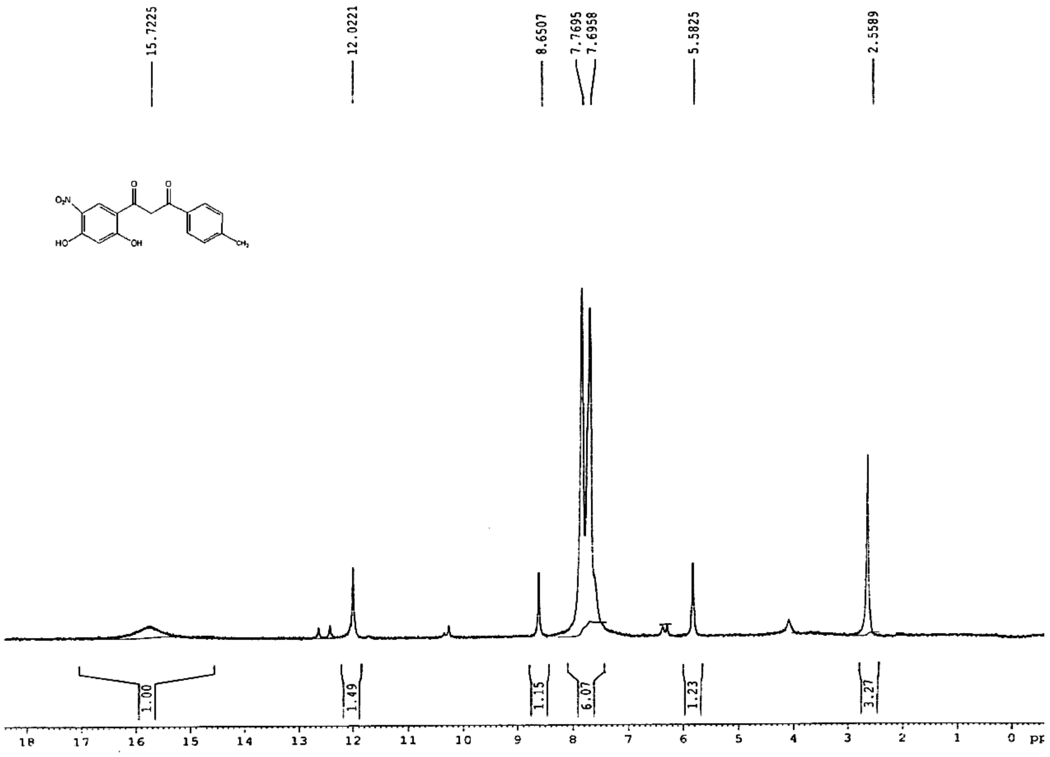

Figure 2: ^{1}H-NMR spectra of DNTD

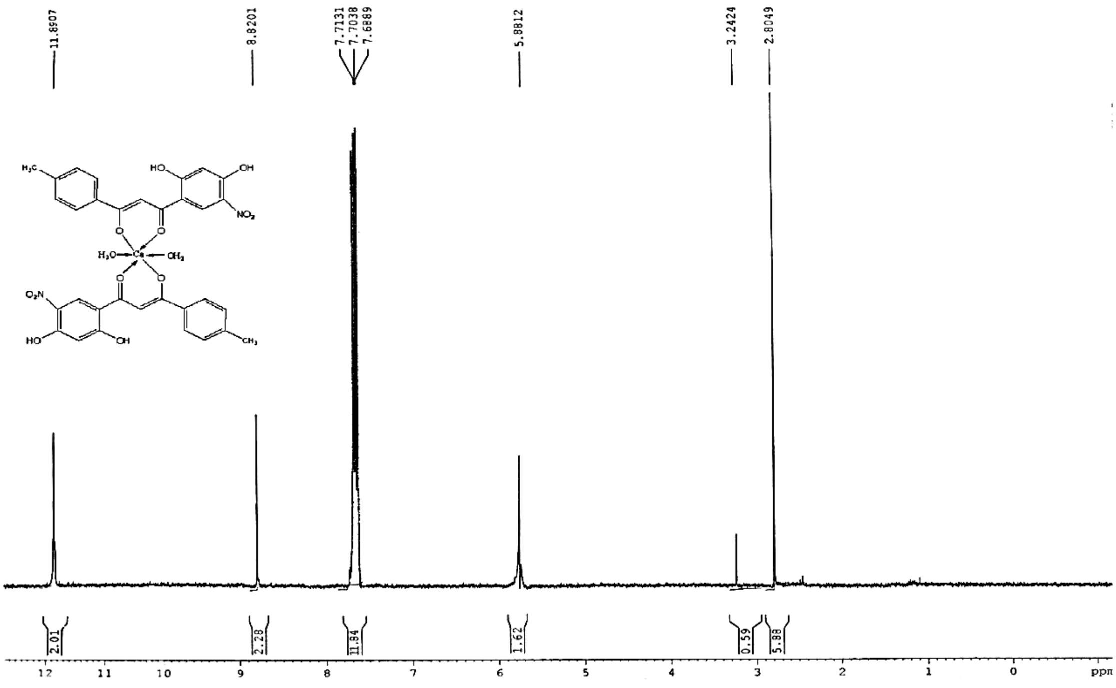

Figure 3: ^{1}H-NMR spectra of Cu(II) DNTD

Spectral analysis: FT-IR spectra were recorded via a KBr disc on a Perkin-Elmer spectrum Rx-I spectrometer. The IR spectra of the ligand and its metal complexes are summarized in table 2. From the close scrutiny of the data depicted in the table 2, it is clearly seen that the band at 1682 cm^{-1} in the case of the chelating ligand may be assigned to the carbonyl group (C=O). This band then shifted towards lower values in case of Mn-(DNTD)$_2$.2H$_2$O to 1608 cm^{-1}, Co- (DNTD)$_2$.2H$_2$O to 1616 cm^{-1}, Zn- (DNTD)$_2$ to 1617 cm^{-1}, Cu- (DNTD)$_2$ to 1618 cm^{-1} and Ni- (DNTD)$_2$.2H$_2$O to 1621 cm^{-1} [26]. This shift indicates that the beta-diketo functionality of the ligand may be coordinated with the transition metal ion through the oxygen atom. The above evidence was further supported by the emergence of new bands at 411 - 470 cm^{-1} in the spectra of the metal complexes, which may be due to the metal–oxygen vibration[8].

The band of (C-O) enolic group which appears at 1202 cm^{-1} in the ligand spectra, was observed to be disappeared completely in the IR spectra of metal-DNTD complex. This is due to disappearance of keto-enol tautomerism in the metal-DNTD complex and formation of metal-Ligand bonding through the oxygen atoms involved in the tautomerism. This supports our earlier observations as evident from emergence of new bands at 411 - 470 cm^{-1}. The other prominent peaks observed in case of both DNTD ligand as well as metal-DNTD complex are as follows.

The band in the range of 1569 cm^{-1} – 1606 cm^{-1} for the C = C group, band in the range of 1189 cm^{-1} – 1221 cm^{-1} for the C - O phenolic group, band gap in the range of 3008 cm^{-1} - 3072 cm^{-1} for the >CH aliphatic group, peak at 3430 cm^{-1} up to 3459 cm^{-1} for the -OH phenolic group, peaks in the range of 1488 cm^{-1} up to 1528 cm^{-1} for the C-NO_2 group whereas the band was observed at 2863 cm^{-1} up to 2879 cm^{-1} for the -C-CH_3 group. Also, one of the observations in case of metal-coordinated H_2O group was its appearance at 765 cm^{-1} approx. in all the metal-complex except in case of Cu-$(DNTD)_2$ and Zn-$(DNTD)_2$[27]. Hence it was concluded that water of hydration may not be present in these complexes.

^{1}H-NMR data were recorded on a Brucker AC-300 F (300 MHz) NMR spectrometer using DMSO-d^6 and $CDCl_3$ as solvents and tetramethylsilane as an internal standard. The ^{1}H-NMR spectrum of DNTD as depicted in fig. 2 shows a singlet at $\delta = 15.72$ ppm for the enolic –OH group, a singlet at $\delta = 12.02$ ppm for the phenolic –OH group near the carbonyl group and a singlet at $\delta = 5.58$ ppm for the remaining –OH group near the –NO_2 group. Multiplets in the region of 7.69 ppm to 7.76 ppm correspond to the presence of aromatic hydrogen. The singlet signal at $\delta = 8.65$ ppm corresponds to the –CH= group. The singlet at $\delta = 2.56$ ppm corresponds to the –CH_3 group. The ^{1}H-NMR spectrum of the copper complex of DNTD at 400 MHz in D_2O has been depicted in fig. 3.

From the close scrutiny, it is observed that it shows no peak at approximately 15.72 ppm, indicating the absence of an enolic –OH group, which implies the deprotonation and coordination of oxygen with the metal ion. This observation is also supported from the IR spectral analysis. The peak for the –CH= proton present in the ligand shifted downfield from 8.65 ppm to 8.82 ppm, which again indicates the coordination of the metal with two carbonyl groups of the ligand. The singlet at $\delta = 11.89$ ppm was assigned to the –OH groups near the carbonyl group and the singlet at $\delta = 5.88$ ppm was assigned to the remaining –OH groups near the –NO_2 group. Multiplets observed in the region from 7.68 ppm to 7.71 ppm correspond to the presence of aromatic protons. The single peak at $\delta = 2.80$ ppm indicates the presence of six protons for the –CH_3 group.

The mass spectrum of DNTD showed a molecular ion peak at 315 m/z and an M^{+1} peak at 316.0 m/z as depicted in fig. 4. Several other peaks were observed at 137 m/z, which is a base peak, 301 m/z, 285, 269 m/z, 120 m/z and 105 m/z. The expected fragmentation pattern of the molecular ion is presented in fig. 4.

UV-Vis absorption spectra were recorded on UV-VIS-NIR Spectrophotometer for the metal complexes of DNTD as in fig. 5. From the close scrutiny of the results collected in table 3, it can be concluded that in case of the Mn-$(DNTD)_2.2H_2O$ complex, absorbance equivalent to 30.21 kK can be due to charge transfer transition. In the case of Co-$(DNTD)_2.2H_2O$ complex, the transitions taking places are due to the possible $^4T_{1g\,(P)} \leftarrow {}^4T_{1g}$ and $^4A_{2g} \leftarrow {}^4T_{1g}$ transitions at 20.16 kK and 13.02 kK respectively. In the case of Ni-$(DNTD)_2.2H_2O$ complex, the transitions taking places are due to the possible $^3T_{1g} \leftarrow {}^3A_{2g}$ and charge transfer transition 16.66 kK and 29.32 kK respectively. In the case of Cu-$(DNTD)_2$ complex, the transitions taking places are due to the possible $^2E_g \leftarrow {}^2B_{1g}$ transitions at 14.79 kK. In the case of Zn-$(DNTD)_2$ complex, the d-d transitions could not be assigned from the spectral analysis and may have charge transfer transitions only.

In electromagnetism, the magnetic susceptibility is the degree of magnetization of a material in response to an applied magnetic field. Most of the transition metal compounds are paramagnetic due to the presence of unpaired electrons. The chemistry of transition metals provides the most interesting field for magnetic investigation. This is due to the fact that the influences of incoming groups on the d electrons of the metal ions are sufficiently strong to affect significantly on their magnetic properties. The study of magnetic properties provides the mechanism of these interactions and can yield valuable information about the bonding and structures of transition metal compounds.

Thus magneto-chemistry is one of the most valuable techniques in the investigations of geometry of transition metal complexes. Bivalent manganese complexes are of both high spin and low spin. They form octahedral, tetrahedral, square planar or low symmetry compounds. Octahedral as well as tetrahedral manganese complexes show magnetic moment near to μeff= 5.92 B.M. independent of temperature.

The magnetic moment of Mn(II) in the range of 5.2-5.9B.M. indicates a high spin octahedral geometry while the higher values are reported to be tetrahedral[6]. The magnetic properties of high spin octahedral Co(II) complexes are governed by the orbitally degenerate term ^4T_g[3]. This provides an orbital contribution to the magnetic moment so that at room temperature, magnetic moment values are found to be in the range of 4.7-5.2BM. Tetrahedral Co(II) complexes generally have values of magnetic moments in the range of 4.3-4.7B.M. and their square planer complexes are reported to be in the range of 2.2-2.9BM[25]. Ni(II) having 3d^8 configuration forms square planer, octahedral or tetrahedral complexes. In octahedral complexes of Ni(II) complexes, magnetic moment lies in the range of 2.98-3.4 B.M.[15] while in tetrahedral complexes, it is around 3.5-4.5 B.M.

Square planer complexes of Ni(II) are usually diamagnetic in nature obtained by the ligands capable of forming a highly covalent bond with a strong σ and π bonding character[16]. Cu(II) complexes are known to have octahedral, distorted octahedral or square planar geometry and the magnetic moment lies between 1.70-2.20 B.M.[23]. Square planar stereochemistry lies around 1.82 BM at room temperature while the higher values are reported to be distorted octahedral. The synthesized Zn(II) complex has been found to be diamagnetic in nature as expected due to complete spin paired state[21].

Thermal analysis: Thermogravimetric analysis was performed on a Perkin Elmer SII Diamond TG/DTA thermogravimetric analyzer with a temperature range of 30-1100 ^{0}C at a heating rate of 10 ^{0}C under atmospheric conditions. The thermal data of the complexes are shown in table 4.

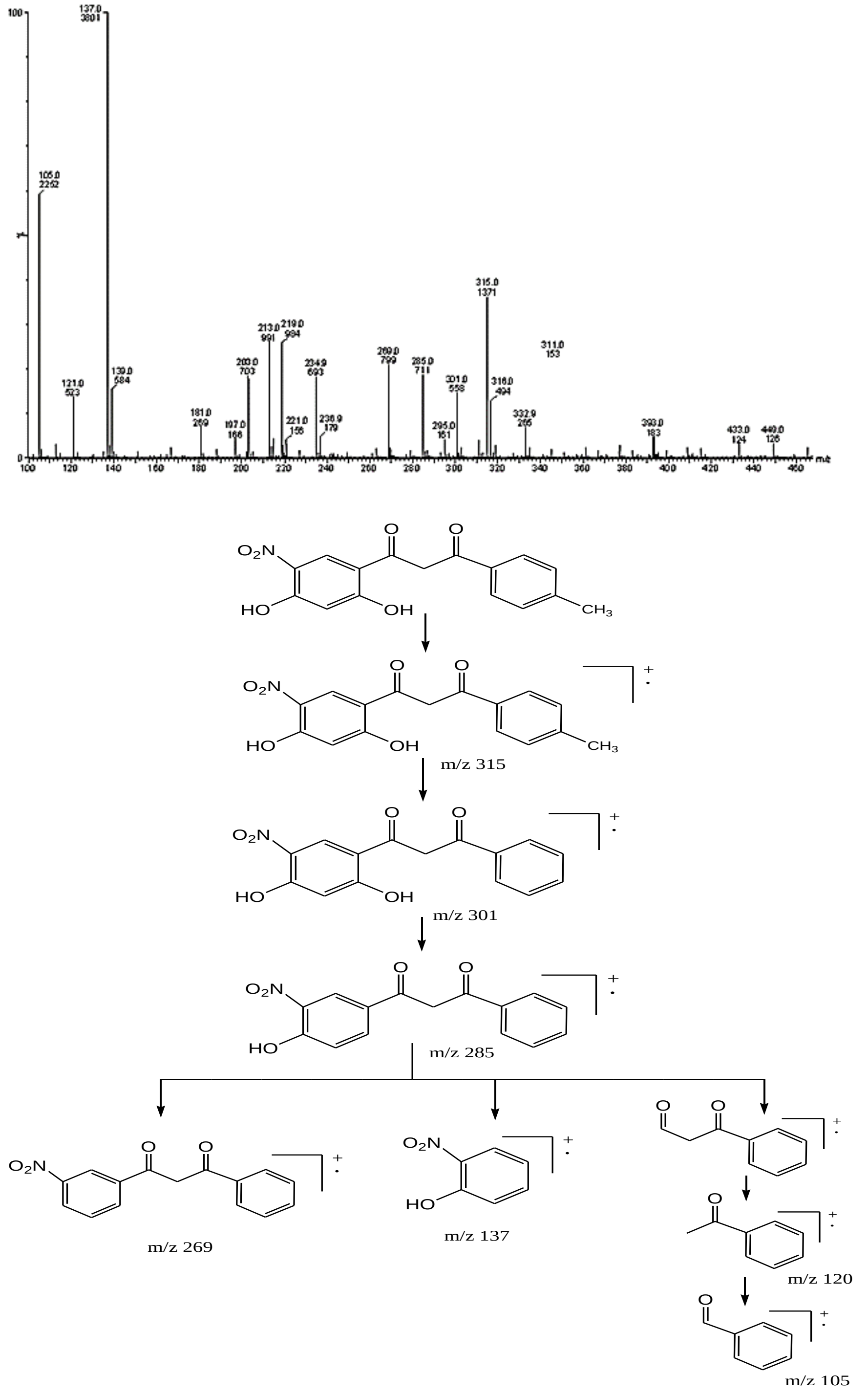

Figure 4: Mass spectra and possible fragmentation pattern of DNTD ligand

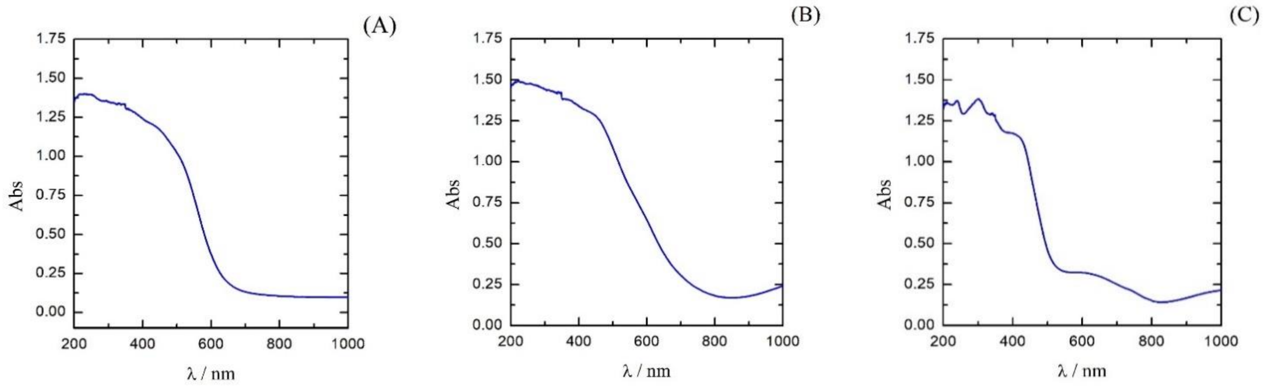

$Mn(DNTD)_2.2H_2O$ **$Co(DNTD)_2.2H_2O$** **$Ni(DNTD)_2.2H_2O$**

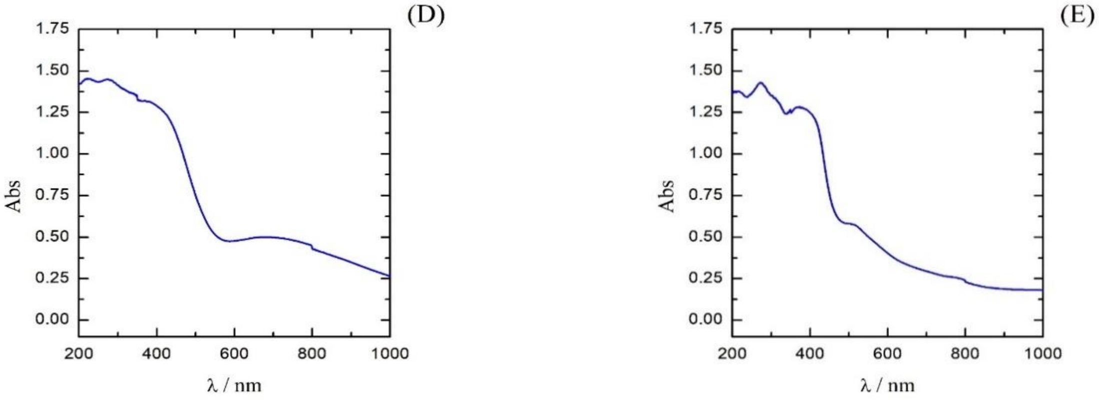

$Cu(DNTD)_2$ **$Zn(DNTD)_2$**

Figure 5: Electronic Spectra of DNTD Metal Complexes

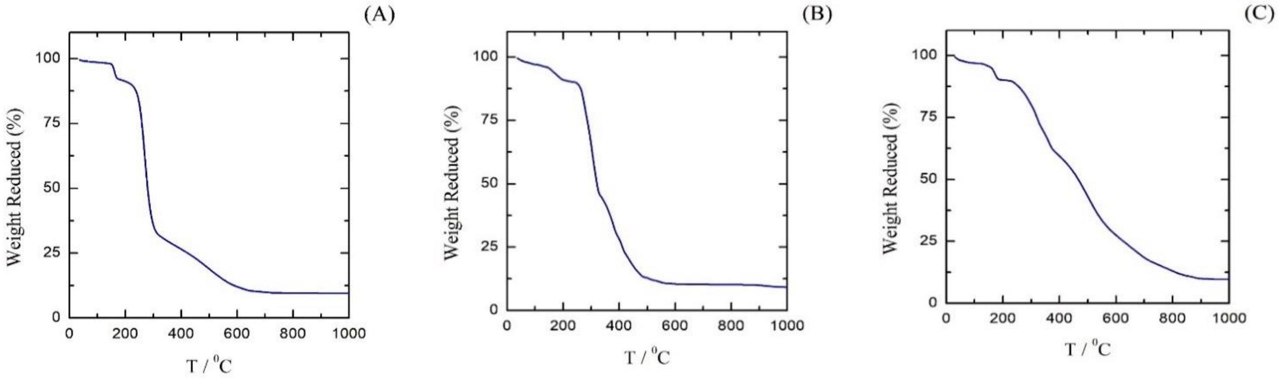

$Mn(DNTD)_2.2H_2O$ **$Co(DNTD)_2.2H_2O$** **$Ni(DNTD)_2.2H_2O$**

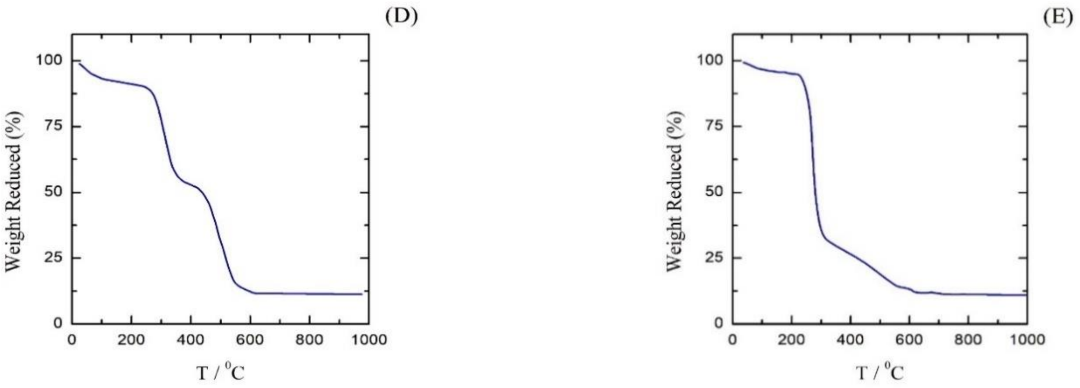

$Cu(DNTD)_2$ **$Zn(DNTD)_2$**

Figure 6: Thermograms of the metal complexes

Table 3
Magnetic and electronic spectral studies

Complex	**Effective Magnetic Moment (μ_{eff})**	**Absorbance (kK)**	**Assignments**	**Stereochemistry**
$Mn(DNTD)_2.2H_2O$	5.78	30.21	Charge Transfer	Octahedral
$Co(DNTD)_2.2H_2O$	4.77	20.16 13.02	$^4T_{1g}(P) \leftarrow {}^4T_{1g}$ $^4A_{2g} \leftarrow {}^4T_{1g}$	Octahedral
$Ni(DNTD)_2.2H_2O$	3.32	16.66 29.32	$^3T_{1g} \leftarrow {}^3A_{2g}$ Charge Transfer	Octahedral
$Cu(DNTD)_2$	1.56	14.79	$^2E_g \leftarrow {}^2B_{1g}$	Square Planar
$Zn(DNTD)_2$	diamagnetic	--	--	Tetrahedral

Table 4
Thermal data of the complexes

S.N.	**Complex**	**Coordination water Obs (calc) (%)**	**Decomposition Temperature (^0C)**	**% Weight loss Obs (calc)**
1.	$Mn(DNTD)_2.2H_2O$	5.08 (4.99)	431	89.64(90.17)
2.	$Co(DNTD)_2.2H_2O$	5.08 (4.96)	416	89.22(89.67)
3.	$Ni(DNTD)_2.2H_2O$	4.99 (4.96)	570	90.10(89.70)
4.	$Cu(DNTD)_2$	--	420	88.43(88.54)
5.	$Zn(DNTD)_2$	--	421	88.08(88.30)

Thermogravimetric analysis (TGA) serves as a crucial thermal method utilized across research, quality assurance and manufacturing processes[24]. This technique monitors material mass variations related to temperature or time during controlled heating. Its primary applications involve assessing a material's heat resistance and analyzing its constituents, including volatile substances and inorganic fillers. TGA proves highly effective in examining diverse materials, highlighting their unique breakdown behaviors. Dynamic thermogravimetric analysis of all the five complexes Ni(II)-$(DNTD)_2.2H_2O$, Co(II)-$(DNTD)_2.2H_2O$, Mn(II)-$(DNTD)_2.2H_2O$, Cu(II)-$(DNTD)_2$, Zn(II)-$(DNTD)_2$ has been carried out at different temperature ranging from 30 to 1000 ^0C. Degradation pattern of each thermogram of different complexes is also shown in fig. 6.

All the thermograms of complexes show three step degradation including loss of water molecule except the complexes of Cu and Zn which do not contain water of coordination. The high volatility first weight loss step is due to the loss of water molecule from the complex. Weight loss in the second step occurs due to combustion of compounds such as residual carbon from ligand and attached functional groups. The residue value is the remaining ash due to inorganic metallic oxide of material that was present in the complex.

Stepwise decomposition of Ni(II)-$(DNTD)_2.2H_2O$ complex has been shown in fig. 6A. It shows a loss of 4.5 % observed at temperature 140 ^0C which corresponds to loss of water molecule present due to entrapped moisture as well as water molecules in coordination with complex, correlated with theoretical value of 4.97%. After loss of water molecule, thermogram of complex depicts second step of decomposition which is slow and occurs in temp range from 140 ^0C to 830 ^0C corresponding to degradation and combustion of compounds such as residual carbon from ligand and attached functional groups i.e. hydroxyl, methyl and nitro groups linked to aromatic ring showing loss of 88.3% against calculated 89.63% present per repeat unit of ligand. Third step of degradation starts from 830 ^0C to 1010 ^0C which represents the residue value which corresponds to remaining ash due to inorganic metallic oxide of material present in the complex. For Co(II)-$(DNTD)_2.2H_2O$ complex, it has been shown in fig. 6B.

It shows a loss of 3.9% observed at temperature 146 ^0C which corresponds to loss of water molecule present due to entrapped moisture as well as water molecules in coordination with complex and correlated with theoretical value of 4.97%. After loss of water molecule, thermogram of complex depicts second step of decomposition which is slow and occurs in temp range from 146 ^0C to 476 ^0C corresponding to degradation and combustion of compounds such as residual carbon from ligand and attached functional groups i.e. hydroxyl, methyl and nitro groups linked to aromatic ring showing loss of 85.90% against calculated 89.63% present per repeat unit of ligand. Third step of degradation starts from 830 ^0C to 1010 ^0C which represents the residue value which corresponds to remaining ash due to inorganic metallic oxide of material that was present in the complex.

For Mn(II)-$(DNTD)_2.2H_2O$ complex, it has been depicted in fig. 6C. It shows a loss of 5.77% observed at temperature 156 ^0C which corresponds to loss of water molecule present due to entrapped moisture as well as water molecules in coordination with complex and correlated with theoretical value of 5%. After loss of water molecule, thermogram of complex depicts second step of decomposition which is slow and corresponds to degradation and combustion of compounds such as residual carbon from ligand and attached functional groups i.e. hydroxyl, methyl and nitro groups linked to aromatic ring showing loss of 89.32% against calculated 90.40% present per repeat unit of ligand. Third step of degradation starts from 606 ^{0}C to 1006 ^{0}C which represents the residue value which corresponds to remaining ash due to inorganic metallic oxide of material present in the complex.

Stepwise decomposition of Cu(II)-$(DNTD)_2$ complex has been shown in fig. 6D[13]. Copper forms square planer complex without water of coordination. The first step of degradation is slow and results into removal of moisture and melting of complex with a loss of 9.6% observed at temperature 235 ^{0}C. Thermogram of complex depicts second step of decomposition which is also slow and occurs in temp range from 235 ^{0}C to 405 ^{0}C corresponding to the partial degradation value of 47.5% of the ligand moiety of the complex, in which the ligand undergoes an endothermic decomposition which is followed by oxidation of the ligand fragments by atmospheric oxygen.

Third step of degradation results into complete degradation of ligand along with β diketone moiety starting from 405 ^{0}C to 585 ^{0}C with the observed value of 13 % against calculated value of 10.92 %. The last stage from 585 ^{0}C to 975 ^{0}C represents the residue value which corresponds to remaining ash due to inorganic metallic oxide of material present in the complex. Thermal degradation of Zn(II)-$(DNTD)_2$ complex has been shown in fig. 6E[1,5]. Zinc forms tetrahedral complex without water of coordination. The first step of degradation is slow and results into removal of moisture and melting of complex with a loss of 5.1% observed at temperature 216 ^{0}C.

Thermogram of complex depicts second step of decomposition which is also slow and occurs in temp. range from 216 ^{0}C to 306 ^{0}C corresponding to the partial degradation value of 33.70% of the ligand moiety of the complex, in which the ligand undergoes an endothermic decomposition followed by oxidation of the ligand fragments by atmospheric oxygen. Third step of degradation results into complete degradation of ligand along with β diketone moiety starting from 306 ^{0}C to 606 ^{0}C with the observed value of 13% against calculated value of 11.15%. The last stage from 606 ^{0}C to 1006 ^{0}C represents the residue value which corresponds to remaining ash due to inorganic metallic oxide of material present in the complex.

Biological analysis: The experimental results of the antimicrobial activities of all the compounds determined via the filter paper disc diffusion method screened against pathogenic bacteria compared with standard antibiotic drugs ampicillin, gentamicin and erythromycin have been collected in table 5. It can be seen from the table 5 that ligand 4 is found to active against all the Gram-positive as well as Gram-negative bacterial stains. In case of activity against *E. coli*, it is showing very good anti-bacterial activity compared to standard ampicillin and good activity compared to other standard drugs. Its activity against *P. vulgaris* is very good compared to all the three standard drugs. Most of our newly synthesized metal-complexes were also observed to possess very good activity against the *E. coli* Gram-negative bacterial strains compared to the standard drugs, in particular $Ni(DNTD)_2.2H_2O$ and $Cu(DNTD)_2$.

$Cu(DNTD)_2$ was also observed to have good potency against *P. aeruginosa*. $Ni(DNTD)_2.2H_2O$ and $Zn(DNTD)_2$ have shown very good activities against Gram-negative *P. vulgaris* bacterial stains as compared to standard drugs gentamicin and erythromycin as references. $Ni(DNTD)_2.2H_2O$, $Cu(DNTD)_2$ and $Zn(DNTD)_2$ were found to have very good activity against the Gram-positive *B. subtilis* bacterial stains. $Cu(DNTD)_2$ was found to observe very good anti-bacterial activity against *S. aureus* stains compared to the to the standard drugs gentamicin and erythromycin.

The enhanced activity of metal complexes can be understood through Overtone's theory and Chelation principles[27]. Overtone's theory of cell permeability suggests that the lipid membrane surrounding cells facilitates the transport of lipid-soluble substances, making liposolubility a key factor influencing antimicrobial effectiveness.

Table 5
Antibacterial activity of the compounds

Source	**Minimum Inhibitory Concentration (MIC) μgmL^{-1} Diameter of Inhibition Zone (in mm)**				
	Gram-negative			**Gram-positive**	
	E. coli	***P. aeruginosa***	***P. vulgaris***	***B. subtilis***	***S. aureus***
DNTD	21	06	19	08	17
$Mn(DNTD)_2.2H_2O$	24	10	--	06	--
$Co(DNTD)_2.2H_2O$	32	--	08	--	--
$Ni(DNTD)_2.2H_2O$	40	08	22	20	12
$Cu(DNTD)_2$	39	24	14	23	15
$Zn(DNTD)_2$	23	07	20	14	--
Ampicillin	8	--	--	11	25
Gentamicin	28	22	10	16	10
Erythromycin	31	19	08	21	07

Chelation, on the other hand, significantly reduces the metal atom's polarity due to the interaction between the ligand's orbitals and the partial sharing of the metal's positive charge with donor groups. Further, it increases the delocalization of π-electrons over the whole chelate ring and enhances the liphophilicity which enhances the penetration of the complexes. This increased lipophilicity enhances the penetration of the complexes into lipid membrane blocking the metal binding-sites on enzymes of microorganism. These complexes have the potential to disrupt the cell's respiration process, thereby inhibiting protein synthesis and ultimately preventing the organism's continued growth.

Conclusion

In this study, we have successfully synthesized and thoroughly characterized 1-(2,4-dihydroxy-5-nitrophenyl)-3-(p-tolyl)propane-1,3-dione alongside its transition metal complexes, employing advanced techniques such as IR, NMR and mass spectrometry. The functionalized β-diketone molecule demonstrated its role as a bidentate ligand, forming coordination bonds with transition metals through the β-diketo moiety. Co(II), Ni(II) and Mn(II) complexes incorporated two distinct types of water molecules in their coordination sphere, Cu(II) and Zn(II) complexes were devoid of coordinating water.

Based on their electronic configurations and magnetic moment measurements, the geometry of manganese(II), cobalt(II) and nickel(II) complexes was determined to be octahedral, Copper(II) exhibited square planar geometry and zinc(II) revealed a tetrahedral arrangement. Notably, the complexes of cobalt(II), nickel(II), manganese(II) and copper(II) displayed paramagnetic behavior whereas the zinc(II) complex was identified as diamagnetic. Furthermore, these synthesized compounds underwent *in vitro* antibacterial testing, showing promise as potential new antimicrobial agents.

Acknowledgement

Our sincere thanks go to Dr. H. D. Juneja, Retired Professor and Ex-Head, Department of Chemistry, Rashtrasant Tukadoji Maharaj Nagpur University, Nagpur for his valuable guidance during the research work and for providing all the necessary facilities.

References

1. Al-Anber M.A., Synthesis and Thermal Properties of Nickel Β-diketonate Polymers, *Oriental Journal of Chemistry*, **29(3)**, 829–836 **(2013)**

2. Clegg J.K., Li F. and Lindoy L.F., Oligo-β-diketones as versatile ligands for use in metallo-supramolecular chemistry: Recent progress and perspectives, *Coordination Chemistry Reviews*, **455**, 214355 **(2022)**

3. De Bruecker L. and Van Speybroeck V., Influence of Number of Ligands and Point Group on the Electronic Structure of Co^{2+} Aqua-Complexes, *Inorganic Chemistry*, **61(51)**, 20743–20756 **(2022)**

4. de Gonzalo G. and Alcántara A.R., Recent Developments in the Synthesis of β-Diketones, *Pharmaceuticals*, **14(10)**, 1043 **(2021)**

5. Dziewulska-Kułaczkowska A., Thermal and spectral studies of Mn(II), Co(II), Ni(II), Cu(II) and Zn(II) complexes with 3-(anilinomethylene)-2-methoxychroman-4-one, *Journal of Thermal Analysis and Calorimetry*, **109**, 7–15 **(2012)**

6. El-Ghamry M.A., Elzawawi F.M., Aziz A.A.A., Nassir K.M. and Abu-El-Wafa S.M., New Schiff base ligand and its novel Cr (III), Mn (II), Co (II), Ni (II), Cu (II), Zn (II) complexes: spectral investigation, biological applications and semiconducting properties, *Scientific Reports*, **12(1)**, 17942 **(2022)**

7. Fathima A.A., Kumaravel V., Jonathan D.R., Sadasivam S.K., Yuvashri R. and Usha G., Synthesis, structural examination, molecular interaction analysis, in vitro and in silico anticancer activity investigation of a new curcumin derivative: 1-(4-chlorobenzoyl)-3,5-bis-((E)-4-methoxy-benzylidene)piperidin-4-one, *Chemical Physics Impact*, **8**, 100559 **(2024)**

8. Ferraro J.R. and Walker W.R., Infrared spectra of hydroxy-bridged copper (II) compounds, *Inorganic Chemistry*, **4(10)**, 1382–1386 **(1965)**

9. Hansen P.E., Tautomerism of β-Diketones and β-Thioxoketones, *Encyclopedia*, **3(1)**, 182–201 **(2023)**

10. Hansen P.E., Structural studies of β-diketones and their implications on biological effects, *Pharmaceuticals*, **14(11)**, 1189 **(2021)**

11. Jacinto F.E., de Oliveira L.P., Batista A.A., Oliveira K.M. and Correa R.S., Ruthenium (II) complexes of curcumin and β-diketone derivatives: effect of structural modifications on their cytotoxicity, *Royal Society Open Science*, **11(7)**, 240353 **(2024)**

12. Kaur N., Grewal P. and Poonia K., Dicarbonyl compounds in O-heterocycle synthesis, *Synthetic Communications*, **51(16)**, 2423–2444 **(2021)**

13. Kavitha N. and Lakshmi P.V.A., Synthesis, characterization and thermogravimetric analysis of Co(II), Ni(II), Cu(II) and Zn(II) complexes supported by ONNO tetradentate Schiff base ligand derived from hydrazinobenzoxazine, *Journal of Saudi Chemical Society*, **21(1)**, S457–S466 **(2017)**

14. Kumar A. and Sridharan V., Transition Metal-Catalyzed Synthesis of 1, 2-Diketones: An Overview, *Asian Journal of Organic Chemistry*, **10(7)**, 1619–1637 **(2021)**

15. Lever A.B.P., The magnetic moments of some tetragonal nickel complexes, *Inorganic Chemistry*, **4(5)**, 763–764 **(1965)**

16. Manimaran P., Balasubramaniyan S., Azam M., Rajadurai D., Al-Resayes S.I., Mathubala G., Manikandan A., Muthupandi S., Tabassum Z. and Khan I., Synthesis, spectral characterization and biological activities of Co (II) and Ni (II) mixed ligand complexes, *Molecules*, **26(4)**, 823 **(2021)**

17. Mohabe P., Yadao B., Pandhurnekar H., Bhattacharya D. and Naktode R., Synthesis and Antibacterial Screening of Metal β-diketonates, *International Journal of Scientific Research in Science and Technology*, **9**, 384–392 **(2021)**

18. Mohareb R.M., Megally Abdo N.Y. and Al-darkazali W.N., Uses of cyclohexan-1, 3-dione for the synthesis of thiazole, pyrazole, thiophene, isoxazole and pyran derivatives with antitumor activities, *Letters in Drug Design & Discovery*, **17(5)**, 597–609 **(2020)**

19. Nehra K., Dalal A., Hooda A., Bhagwan S., Saini R.K., Mari B., Kumar S. and Singh D., Lanthanides β-diketonate complexes as energy-efficient emissive materials: A review, *Journal of Molecular Structure*, **1249**, 131531 **(2022)**

20. Pellei M., Caviglia M., Karade D.V., Gandin V., Marzano C., Poyil A.N., Dias H.R. and Santini C., Synthesis and cytotoxicity studies of Cu (I) and Ag (I) complexes based on sterically hindered β-diketonates with different degrees of fluorination, *Dalton Transactions*, **52(34)**, 12098–12111 **(2023)**

21. Prasad R.N., Agrawal M. and George R., Mixed-Ligand Complexes of Ni (II), Cu (II) and Zn (II) with 5-Chlorosalicylaldehyde and β-Diketones, *Synthesis and Reactivity in Inorganic and Metal-Organic Chemistry*, **34(5)**, 943–952 **(2004)**

22. Priya N.P., Arunachalam S.V., Sathya N., Chinnusamy V. and Jayabalakrishnan C., Catalytic and antimicrobial studies of binuclear ruthenium(III) complexes containing bis-β-diketones, *Transition Metal Chemistry*, **34**, 437–445 **(2009)**

23. Rao B.V. and Puri D.M., Copper (II) Complexes of Organo-phosphonic Acids-A Comparative Study, *Journal of Chemistry*, **8**, S271–S281 **(2011)**

24. Sadaka Shehin M.C., Jayaraj K.A., Ummath Ameen, Sasidharan Venu and Parveen Fahmeeda P.S., Isolation and Identification of Biofilm forming Bacteria from Glass Panels exposed in Sea Waters of South Andaman, India, *Res. J. Biotech.*, **19(4)**, 54–63 **(2024)**

25. Sahu P.K., Kharel R., Shome S., Goswami S. and Konar S., Understanding the unceasing evolution of Co (II) based single-ion magnets, *Coordination Chemistry Reviews*, **475**, 214871 **(2023)**

26. Sheikh J., Juneja H., Ingle V., Ali P. and Hadda T.B., Synthesis and in vitro biology of Co (II), Ni (II), Cu (II) and Zinc (II) complexes of functionalized beta-diketone bearing energy buried potential antibacterial and antiviral O, O pharmacophore sites, *Journal of Saudi Chemical Society*, **17(3)**, 269–276 **(2013)**

27. Świderski G., Jabłońska-Trypuć A., Kalinowska M., Świsłocka R., Karpowicz D., Manuszewska M. and Lewandowski W., Spectroscopic, theoretical and antioxidant study of 3d transition metals (Co (II), Ni (II), Cu (II), Zn (II)) complexes with cichoric acid, *Materials*, **13(14)**, 3102 **(2020)**

28. Verma P.N. and Juneja H.D., Synthesis and characterization of 1-(2′, 4′-dihydroxy-5-nitrophenyl)-3(pyridin-3-yl)-propane-1, 3-dione and its metal complexes, *Journal of Chem. Tech. Research*, **4**, 1000–1006 **(2012)**.

(Received 20th July 2025, accepted 22nd September 2025)